MATHEMATICAL MODELING AND COMPUTING, Vol. 11, No. 4, pp. 1211–1220 (2024)

Mathematical modeling and computer simulation of locomotion conditions of vibration-driven robots

Korendiy V., Kachur O., Kyrychuk V., Markovych B.

Lviv Polytechnic National University,
12 S. Bandera Str., 79013, Lviv, Ukraine

(Received 8 March 2024; Revised 20 November 2024; Accepted 22 November 2024)

This paper investigates the dynamic behavior and locomotion characteristics of vibration-driven robots with wheeled chassis, focusing on the comparison of two types of vibration exciters: a solenoid-type actuator and a centrifugal (inertial) exciter. The research methodology involves 3D modeling using SolidWorks software to design the robots, numerical modeling in Mathematica software to simulate their motion and predict kinematic characteristics, and computer simulation in SolidWorks Motion software to validate the modeling results. The robots utilize overrunning clutches to ensure unidirectional wheel rotation and achieve forward motion through the principle of pure vibratory and vibro-impact locomotion. The influence of excitation frequency and operational parameters on the robot's speed, acceleration, and displacement is analyzed for both types of exciters. The results demonstrate the effectiveness of both solenoid and centrifugal exciters in achieving locomotion, with the centrifugal exciter generally providing lower speeds due to utilizing pure vibration excitation and the solenoid-type actuator offering larger speeds due to operating at vibro-impact conditions. The findings of this study are valuable for researchers and engineers working on the design and optimization of vibration-driven robots for various applications, including pipeline inspection, cleaning, and navigation in challenging environments.

Keywords: *mathematical model; computer simulation; electromagnetic exciter; unbalanced rotor; locomotion characteristics; dynamic diagram; mobile robotics; wheeled chassis; overrunning clutch.*

2010 MSC: 70E55, 70E60 **DOI:** 10.23939/mmc2024.04.1211

1. Introduction

Mobile robotics is a rapidly evolving field with diverse applications ranging from industrial automation to the exploration of hazardous environments. Among the various locomotion mechanisms employed in mobile robots, vibration-driven systems have garnered significant attention due to their simplicity, robustness, and ability to traverse challenging terrains [1,2]. These systems utilize the principle of converting vibrational energy into directional motion, often through asymmetric frictional forces between the robot and the surface on which it moves [3]. This type of locomotion is particularly advantageous in small-scale robots or those operating in confined environments where conventional locomotion mechanisms may be impractical [4].

The fundamental concept of vibration-driven locomotion has been explored in numerous studies. For instance, Du et al. [5] conducted experiments on vibration-driven stick-slip locomotion, providing insights into the sliding bifurcation perspective. Xu and Fang [6] reviewed recent advancements in vibration-driven locomotion systems, highlighting their potential for improved performance. Further research has delved into specific aspects of vibration-driven systems, such as the dynamics and motion control of capsule robots [7], bifurcation analysis of stick-slip motion [8], and optimization strategies for enhancing locomotion performance [9,10]. The influence of friction on vibro-impact locomotion systems has also been investigated [11], emphasizing its crucial role in the dynamic response and motion control of these robots.

This paper focuses on two specific types of vibration-driven robots: one actuated by a solenoid-type actuator and the other by an unbalanced rotor. Previous studies have explored the implementation of unbalanced rotors in vibration-driven robots for various applications, including in-pipe inspection [13,14]. Loukanov et al. [15–17] investigated the dynamic characteristics of vibration-driven robots with unbalanced rotors, contributing valuable insights to the field. The use of solenoid-type actuators in vibration-driven systems has also been investigated, with a focus on their dynamic behavior and operational conditions [18]. Demarchi et al. [19] focused on modeling a solenoid's valve movement, while others have explored the broader applications of solenoids in locomotion and manipulation systems.

The primary objective of this paper is to present a comprehensive analysis of the locomotion conditions of vibration-driven robots with these two distinct excitation mechanisms. The study employs mathematical modeling, computer simulation, and experimental testing to evaluate and compare the performance of each robot design [20, 21]. The findings of this research contribute to the understanding and development of vibration-driven robots for diverse applications, including pipeline inspection [22–25], cleaning, and exploration of confined or hazardous spaces. The research also builds upon previous work on the mathematical modeling and analysis of vibro-impact locomotion systems [26,27], as well as the development of control systems for vibratory machines and vibration isolators [28]. Furthermore, it considers the insights gained from studies on solenoid and piezoelectric actuators design and modeling [29, 30], particularly, implemented in the drives of the wheeled vibration-driven robots [31].

2. Research methodology

This study employs a comprehensive research methodology that integrates mathematical modeling and computer simulation to thoroughly investigate the locomotion characteristics of vibration-driven robots with two distinct excitation mechanisms: a solenoid-type actuator and an unbalanced rotor. This multifaceted approach enables a detailed analysis and comparison of the dynamic behavior and performance of each robot design.

Mathematical modeling methods are used to develop dynamic diagrams and derive motion equations for both robot designs, taking into account the specific characteristics of each excitation mechanism. Computer simulation utilizes SolidWorks software to create 3D models and simulate the robot's locomotion under different operational conditions.

This integrated research methodology enables a comprehensive analysis of the locomotion conditions of the two vibration-driven robot designs. The combination of mathematical modeling and computer simulation provides a robust framework for evaluating the performance, efficiency, and controllability of each robot, contributing valuable insights to the field of vibration-driven robotics.

3. 3D models of the vibration-driven robots

The wheeled robot depicted in Figure 1 is designed for movement across a horizontal surface using vibrations generated by a solenoid (12). Its frame (8) supports four wheels (1) connected to axles (2) via overrunning clutches (3). These clutches permit the wheels to rotate in only one direction, ensuring the robot's forward motion under the action of vibrations. A solenoid (12) is mounted on a plate (9) attached to the frame (8); its plunger (13) periodically strikes a rubber buffer (10), creating an impulse for movement. The design also incorporates bearings (5) for smooth wheel rotation, clamps (6, 7) to secure the wheels to the axles and the axles to the frame, and a return spring (14) that resets the solenoid's plunger (13) after each impact. This configuration efficiently converts vibrational energy into translational motion while maintaining the simplicity and compactness of the robot.

Figure 2 illustrates a wheeled vibration-driven robot propelled by an unbalanced rotor. The robot consists of a body (8) with four rubber wheels (1). The wheels are mounted on axles (2) with overrunning clutches (3) that allow unidirectional rotation. This ensures the robot moves in a single direction despite the oscillating motion of the vibration exciter. Ball bearings (5) are used for smooth wheel rotation and to support additional load. Clamps (6, 7) secure the wheels to the axles and the axles to

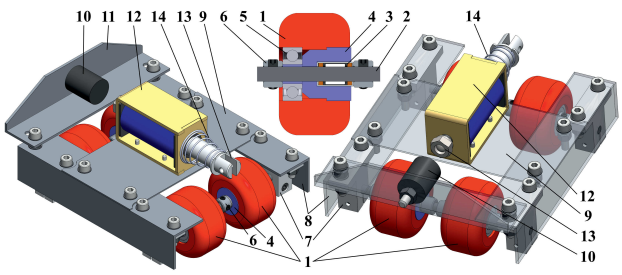

Fig. 1. 3D model of the wheeled vibration-driven robot actuated by a solenoid-type exciter.

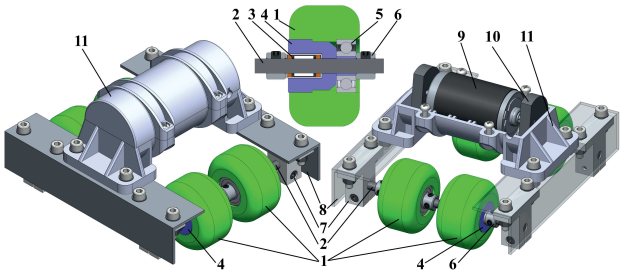

Fig. 2. 3D model of the wheeled vibration-driven robot actuated by an unbalanced rotor.

the robot's body. A DC electric motor (9) with an unbalanced rotor (10) is housed within a casing (11) fixed to the robot's body. The centrifugal forces generated by the rotating unbalanced mass act upon the robot's body, causing a pushing effect. When the direction of these forces aligns with the permitted direction of rotation by the clutches, the robot moves forward. In the opposite direction, the clutches block the wheels, keeping the robot stationary.

4. Dynamic diagrams of the corresponding mechanical oscillatory systems

The dynamic diagram shown in Figure 3 represents a simplified model of the robot's oscillatory system with a solenoid-type exciter. The robot, depicted as a rigid body with mass m_1, moves along the horizontal axis Ox, and its displacement is described by the generalized coordinate x_1. The robot locomotion is induced by an actuating force $F(t)$, generated by a solenoid, which acts upon a smaller mass m_2. This mass is connected to the robot's body through a spring with stiffness k_1. The diagram also includes an inertial coordinate system xOy associated with the stationary surface. The generalized coordinate x_2 represents the absolute displacement of the smaller mass m_2 relative to the inertial coordinate system. The impact interaction between the mass m_2 and the robot's body is modeled by a spring with stiffness k_2. This impact occurs when the difference between displacements x_2 and x_1 exceeds the impact gap δ. The wheels of the robot are equipped with overrunning clutches, allowing them to rotate freely in one direction (clockwise in this case) and lock in the opposite direction. This mechanism ensures the robot's unidirectional motion along the positive direction of the Ox axis.

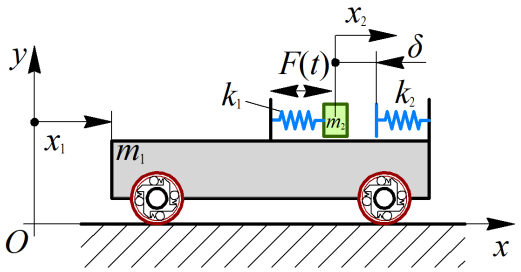

Fig. 3. Simplified dynamic diagram of the robot's mechanical oscillatory system with a solenoid-type exciter.

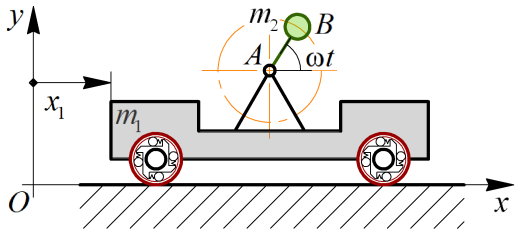

Fig. 4. Simplified dynamic diagram of the robot's mechanical oscillatory system with a centrifugal exciter.

Figure 4 presents a simplified dynamic diagram of the robot's mechanical system with a centrifugal exciter. The robot, with mass m_1, moves along a straight horizontal surface. Its motion is driven by centrifugal forces generated by a rotating mass, m_2, which revolves around a hinge A at a constant angular speed ω. This rotating mass is connected to the robot's body by an eccentric rod AB of length r. The diagram also depicts an inertial coordinate system xOy, associated with the stationary surface, and a generalized coordinate x_1, which describes the robot's horizontal displacement. The wheels are linked to the robot's body through overrunning (free-wheel) clutches, designed to engage in one direction and remain free in the other. This mechanism allows the wheels to rotate clockwise, facilitating the robot's rightward motion. Leftward movement is restricted as the clutches lock and prevent the wheels from rotating in that direction.

5. Mathematical models describing the robots' locomotion conditions

Using the D'Alembert's principle, let us derive the following differential equations describing the locomotion conditions of the wheeled vibration-driven robot with a solenoid-type exciter (see Figure 3):

$$(m_1+m_2)\cdot\ddot{x}_1(t)+(x_1(t)-x_2(t))\cdot k_1+(\delta_0-(x_2(t)-x_1(t)))\cdot k_2^*(t)=F(t)-F_{\text{fr}}(t), \tag{1}$$

$$m_2\cdot\ddot{x}_2(t)+(x_2(t)-x_1(t))\cdot k_1-(\delta_0-(x_2(t)-x_1(t)))\cdot k_2^*(t)=-F(t), \tag{2}$$

where δ_0 is the initial impact gap or the initial distance between the oscillating mass m_2 and the impact plate of the spring k_2 at the equilibrium conditions (state of rest) of the oscillatory system,

$$k_2^*(t)=\begin{cases} k_2, & (x_2(t)-x_1(t))\geqslant\delta_0,\\ 0, & (x_2(t)-x_1(t))<\delta_0,\end{cases} \tag{3}$$

$$F_{\text{fr}}(t)=\begin{cases} 0, & \text{sign}\,(\dot{x}_1(t))\geqslant 0,\\ F(t)-(x_1(t)-x_2(t))\cdot k_1+(\delta_0-(x_2(t)-x_1(t)))\cdot k_2^*(t), & \text{sign}\,(\dot{x}_1(t))<0.\end{cases} \tag{4}$$

Equations (1) and (2) represent the differential equations of motion for the robot's body (mass m_1) and the smaller disturbing mass (mass m_2) connected to the solenoid plunger, respectively. These equations consider the forces acting on each mass, including inertial forces, spring forces, actuation force of the solenoid ($F(t)$), and friction force ($F_{\text{fr}}(t)$). The latter is acting between the robot's wheels and the supporting surface. Equation (3) defines the impact conditions between the smaller mass (m_2) and the robot's body (mass m_1). The corresponding conditions are modeled as a spring with stiffness k_2 that engages only when the displacement $(x_2(t)-x_1(t))$ exceeds the initial impact gap δ_0. Equation (4) describes the friction force ($F_{\text{fr}}(t)$) acting on the robot's body through its wheels. This force is dependent on the direction of the robot's motion $\text{sign}\,(\dot{x}_1(t))$ and is defined differently for positive and negative velocities. When the robot is attempting to move in a forward (rightward) direction, the friction force equals zero, while the friction force expression for the robot's backward (leftward) locomotion is equal to the sum of all the active forces exerted on the robot's body.

In essence, the deduced model captures the complex interplay of forces and impacts that drive the robot's motion. By solving these differential equations, one can analyze the robot's dynamic behavior, predict its locomotion characteristics, and optimize its design for various applications.

Considering the robot's mechanical system with a centrifugal exciter, specifically an unbalanced rotor (see Figure 4), let us also utilize the D'Alembert's principle to derive the following differential equation governing the robot's locomotion:

$$(m_1+m_2)\cdot\ddot{x}_1(t)=F_c(t)-F_{\text{fr}}(t), \tag{5}$$

where the centrifugal force ($\text{F}F_c(t)$) acting on the unbalanced rotor at its steady-state rotation (with constant angular speed) can be described as follows:

$$F_c(t)=m_2\cdot r\cdot\omega^2\cdot\cos\left(\omega\cdot t\right), \tag{6}$$

where r is the eccentricity of the unbalanced rotor (or the length of the rod AB in Figure 4); $F_{\text{fr}}(t)$ is the friction force that is described by the following equation:

$$F_{\text{fr}}(t)=\begin{cases} 0, & \text{sign}\,(\dot{x}_1(t))\geqslant 0,\\ F_c(t), & \text{sign}\,(\dot{x}_1(t))<0.\end{cases} \tag{7}$$

Equation (5) represents the equation of motion for the entire robot system, which includes the robot's body (mass m_1) and the rotating mass (mass m_2). This equation considers the forces influencing the system's movement: inertial force, which represents the combined inertia of the robot's body and the rotating mass; centrifugal force, which represents the force generated by the rotating mass (m_2) due to its eccentric motion (with eccentricity r and angular speed ω). This force acts as the driving force for the robot's locomotion; friction force ($F_{\text{fr}}(t)$) that opposes the robot's motion. Equation (7) describes the friction force ($F_{\text{fr}}(t)$) acting on the robot's body through its wheels. This force is defined as a piecewise function dependent on the direction of the robot's velocity. When $\text{sign}\,(\dot{x}_1(t))\geqslant 0$, this implies the robot is moving to the right (or stationary). In this case, the friction force is considered negligible. This simplification might be based on the assumption that the friction force is relatively

small compared to the driving centrifugal force when the robot moves in the intended direction. When $\text{sign}\,(\dot{x}_1(t)) < 0$, this implies the robot is attempting to move to the left. In this scenario, the friction force is equal to the centrifugal force ($F_c(t)$). This effectively cancels out the centrifugal force, preventing the robot from moving backward. This behavior is consistent with the presence of overrunning clutches in the robot's wheels, which lock and prevent reverse rotation.

The considered friction model captures the effect of the overrunning clutches, allowing forward motion driven by the centrifugal force while preventing backward motion. This simplified representation of friction helps in understanding the fundamental dynamics of the robot's locomotion without delving into complex friction models. In essence, the deduced model simplifies the robot's dynamics by considering the combined effect of the robot's body and the rotating mass as a single unit. The centrifugal force generated by the rotating mass is the primary driver of motion, while the friction force acts as resistance. By solving this differential equation, one can analyze the robot's motion characteristics, predict its behavior under different operating conditions (varying rotor speeds and friction), and optimize its design for specific applications.

6. Numerical modeling of locomotion conditions of the considered vibration-driven robots in Mathematica software

Wolfram Mathematica likely utilizes numerical methods like the Runge–Kutta methods to solve the differential equations governing the robot's motion. These methods provide accurate and stable solutions for dynamic systems, especially those with periodic forcing functions like the centrifugal or solenoid-type exciter in this study. Specifically, the NDSolve function in Mathematica is a powerful tool for solving differential equations numerically, and it employs an adaptive step size control algorithm to ensure accuracy and efficiency.

While carrying out numerical modeling, the following input parameters of the wheeled vibration-driven robots have been adopted based on the corresponding 3D models developed in the SolidWorks software: $m_1 = 1.05\,\text{kg}$, $m_2 = 0.1\,\text{kg}$, $r = 0.028\,\text{m}$, $\delta_0 = 0.009\,\text{m}$. The studied forced frequencies are 3 Hz, 6 Hz, and 9 Hz – for the case of centrifugal exciter, and 6 Hz – for solenoid-type exciter due to the large duration of numerical solving of the corresponding system of differential equations (1) and (2). The amplitude value of the solenoid push-pull force was assumed to be equal to that of the centrifugal force of the unbalanced rotor. In order to obtain the vibro-impact working regimes of the solenoid-type exciter, the following stiffness coefficients were considered: $k_1 = 22\,\text{H/m}$, $k_1 = 10^3\,\text{H/m}$.

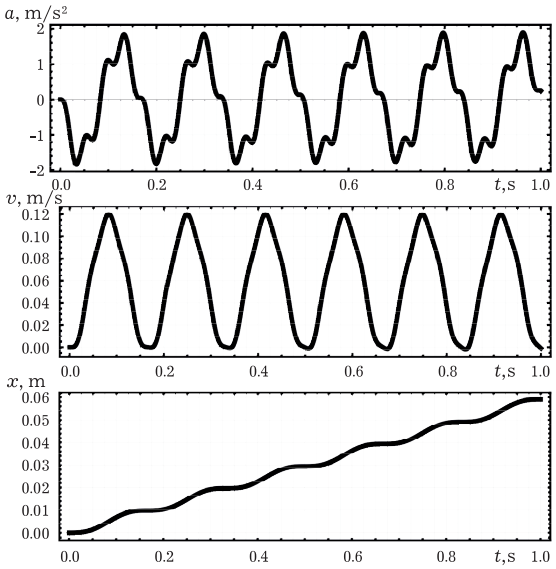

Fig. 5. Results of mathematical modeling of locomotion conditions of the wheeled vibration-driven robot with a solenoid-type exciter.

The Wolfram Mathematica modeling results shown in Figure 5 illustrate the locomotion characteristics of the wheeled vibration-driven robot with a solenoid-type exciter. The model, based on the differential equations (1) and (2) describing the robot's motion, provides insights into how the robot's acceleration, speed, and displacement vary over time due to the solenoid actuation. The upper graph displays a pulsating pattern with distinct peaks and troughs, indicating rapid changes in acceleration caused by the solenoid's plunger impacts. The acceleration of the robot's body fluctuates between approximately $-2\,\text{m/s}^2$ and $2\,\text{m/s}^2$. The non-symmetrical nature of the acceleration profile is due to the impact and return phases of the solenoid actuation. The speed graph exhibits a fluctuating pattern with an overall increasing trend. This suggests that the robot maintains a net forward motion despite the intermittent accelerations and decelerations caused

by the solenoid. The speed varies between 0 m/s and about 0.12 m/s, with the peaks corresponding to the instances of positive acceleration. The displacement graph clearly shows the robot's continuous forward movement over time. The upward trend of the graph confirms the successful conversion of the vibrational energy from the solenoid actuator into directed locomotion. Over the simulated time frame of 1 second, the robot achieves a displacement of roughly 0.06 m.

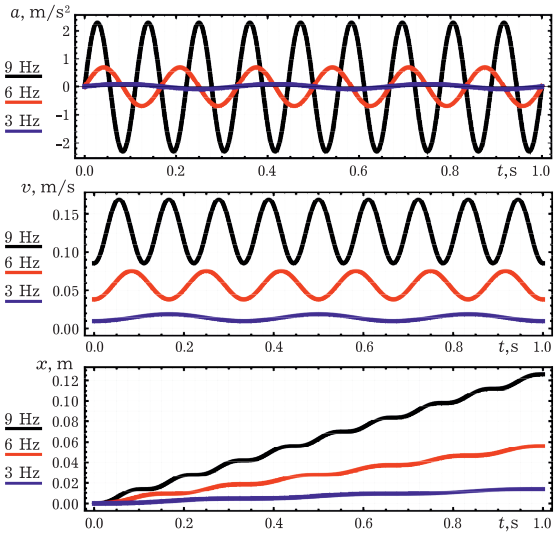

Fig. 6. Results of mathematical modeling of locomotion conditions of the wheeled vibration-driven robot with a centrifugal exciter.

The Wolfram Mathematica modeling results shown in Figure 6 illustrate the locomotion characteristics of the wheeled vibration-driven robot with a centrifugal exciter under different excitation frequencies (3 Hz, 6 Hz, and 9 Hz). The model, based on the differential equation (5) describing the robot's motion, provides insights into how the robot's acceleration, speed, and displacement vary over time with changes in the unbalanced rotor's speed. The upper graph shows a consistent sinusoidal pattern for each frequency, indicating periodic changes in the robot's acceleration. The amplitude of acceleration increases with higher frequencies, suggesting a stronger driving force from the centrifugal exciter. For instance, at 3 Hz, the acceleration fluctuates between approximately $-0.08\,\mathrm{m/s^2}$ and $0.08\,\mathrm{m/s^2}$, while at 9 Hz, it ranges from $-2.3\,\mathrm{m/s^2}$ to $2.3\,\mathrm{m/s^2}$. The speed graphs exhibit a fluctuating pattern with an overall increasing trend for all frequencies. This indicates that the robot maintains a net forward motion despite the oscillations. Higher frequencies lead to more pronounced fluctuations in speed and a higher average speed. At 3 Hz, the speed varies between 0 m/s and roughly 0.02 m/s, whereas at 9 Hz, it ranges from 0.086 m/s to approximately 0.17 m/s. The displacement graphs clearly demonstrate the robot's continuous forward movement over time. The slope of each curve represents the average speed, which increases with higher excitation frequencies. This confirms that the robot effectively converts the vibrational energy into directional motion, and higher frequencies result in faster locomotion. For example, at 3 Hz, the robot travels approximately 0.014 m in 1 second, while at 9 Hz, it covers around 0.126 m in the same time frame. Considering the excitation frequency of 6 Hz, the robot's acceleration oscillates between roughly $-0.68\,\mathrm{m/s^2}$ and $0.68\,\mathrm{m/s^2}$; the speed fluctuates between 0.4 m/s and about 0.75 m/s; in 1 second, the robot travels approximately 0.056 meters.

7. Computer simulation of the robots' locomotion in SolidWorks Motion software

SolidWorks Motion employs a numerical solver to simulate the robot's motion. This solver utilizes a time-stepping approach to calculate the robot's position, velocity, and acceleration at discrete time intervals. The specific numerical method used in SolidWorks Motion is typically a variation of the Runge–Kutta method, which is a widely used technique for solving ordinary differential equations. This method provides accurate and stable solutions for dynamic systems, such as the vibration-driven robot in this study.

The SolidWorks Motion simulation results shown in Figure 7 effectively demonstrate the locomotion characteristics of the wheeled vibration-driven robot with a solenoid-type exciter. The simulation visualizes the robot's movement driven by the periodic impacts of the solenoid actuator. The upper graph exhibits a pulsating pattern with rapid changes in acceleration, reaching peak values of approximately $\pm 2000\,\mathrm{mm/s^2}$ and even more. These sudden changes correspond to the impacts of the solenoid actuator, which impart impulsive forces to the robot's body. The speed graph displays a fluctuating pattern with an overall increasing trend. The speed fluctuates between approximately 0 mm/s and 117 mm/s, indicating that the robot experiences periods of acceleration and deceleration. However,

the net effect is a forward motion with a positive average speed. The displacement graph clearly shows the robot's continuous forward movement over time. The upward trend of the graph confirms the successful conversion of the vibrational energy from the solenoid actuator into directed locomotion. Over a time interval of 3 seconds, the robot achieves a displacement of approximately 175 mm, indicating an average speed of roughly 58 mm/s.

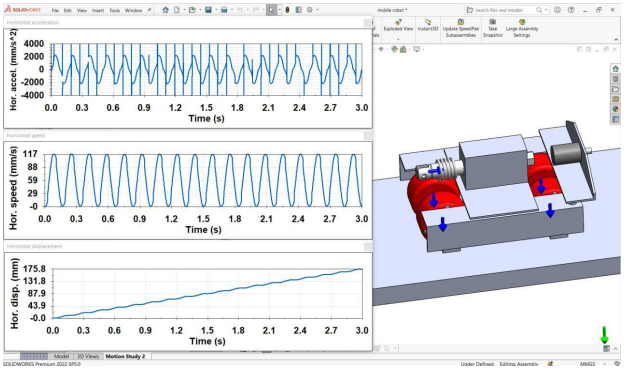

Fig. 7. Results of computer simulation of locomotion conditions of the wheeled vibration-driven robot with a centrifugal exciter.

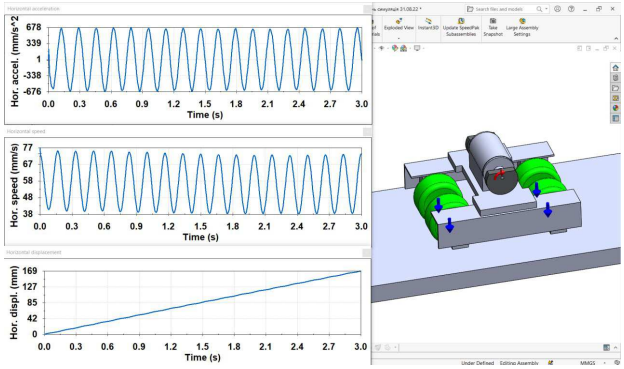

Fig. 8. Results of computer simulation of locomotion conditions of the wheeled vibration-driven robot with a centrifugal exciter.

The SolidWorks Motion simulation results shown in Figure 8 effectively illustrate the locomotion characteristics of the wheeled vibration-driven robot with a centrifugal exciter. The simulation visualizes the robot's movement along a straight line, driven by the centrifugal forces generated by the rotating unbalanced mass. The acceleration graph displays a sinusoidal pattern with peaks reaching approximately $\pm 676\,\mathrm{mm/s^2}$. This periodic change in acceleration is consistent with the nature of the centrifugal force generated by the rotating unbalanced mass. The speed graph shows a fluctuating pattern, ranging from approximately 38 mm/s to 75 mm/s. Despite these fluctuations, the robot maintains a net forward motion, as indicated by the positive average speed. The displacement graph exhibits a clear upward trend, indicating the robot's continuous forward movement. Over a time interval of 3 seconds, the robot covers a distance of approximately 169 mm, resulting in an average speed exceeding 56 mm/s.

8. Discussion of the obtained results

This section generalizes the results obtained from the numerical modeling and computer simulations of the locomotion conditions of the two vibration-driven robot designs.

The Wolfram Mathematica modeling results illustrate the locomotion characteristics of both robot designs under varying excitation frequencies. The model of the robot with a solenoid-type exciter demonstrates the robot's acceleration, speed, and displacement profiles over time. The acceleration graph exhibits a pulsating pattern, the speed graph shows fluctuations with an overall increasing trend, and the displacement graph confirms continuous forward motion. The model of the robot with centrifugal exciter demonstrates the influence of the excitation frequency on the robot's locomotion. Higher frequencies result in faster movement but also more pronounced oscillations in speed and acceleration. The graphs show how the robot's acceleration, speed, and displacement change with varying frequencies.

The SolidWorks Motion simulation results provide a visual representation of the robots' movement and generate graphs illustrating their kinematic characteristics. For the robot with solenoid-type exciter, the simulation results show the robot's horizontal acceleration, speed, and displacement over time. The acceleration graph exhibits a pulsating pattern, the speed graph shows fluctuations with an overall increasing trend, and the displacement graph demonstrates continuous forward motion. Considering the robot with centrifugal exciter, the simulation results show the robot's horizontal acceleration, speed, and displacement over time. The acceleration graph exhibits a sinusoidal pattern, the speed

graph shows fluctuations with an overall increasing trend, and the displacement graph demonstrates continuous forward locomotion.

The results from both numerical modeling and computer simulation demonstrate the effectiveness of both solenoid and centrifugal exciters in achieving locomotion. However, the centrifugal exciter generally provides lower speeds due to utilizing pure vibration excitation, while the solenoid-type actuator offers larger speeds due to operating at vibro-impact conditions. The findings also highlight the influence of excitation frequency and operational parameters on the robot's speed, acceleration, and displacement for both types of exciters. Higher excitation frequencies generally lead to faster locomotion but also more pronounced oscillations in acceleration and speed.

The obtained results are consistent with the findings of other researchers in the field of vibration-driven robotics. For instance, [3, 4, 6, 7] investigated the influence of excitation frequency and friction on the locomotion of vibration-driven robots and observed similar trends in speed and acceleration. The use of overrunning clutches to achieve unidirectional motion has also been explored in various studies, such as [16–18], which reported similar locomotion behaviors. The present study builds upon the authors' previous works [1, 14, 31] by providing a detailed comparative analysis of two distinct excitation mechanisms and their impact on robot locomotion.

Further research can be directed towards optimizing the design and control parameters of the robots to improve their locomotion efficiency and adaptability to different terrains. Investigating the influence of various friction models, exploring different control algorithms, and developing energy-efficient actuation mechanisms are potential avenues for future research. Additionally, the application of these robots in specific tasks, such as pipeline inspection, cleaning, and exploration of hazardous environments, can be further explored.

The vibration-driven robots investigated in this study have potential applications in various fields. Their compact size, simple design, and ability to navigate challenging terrains make them suitable for tasks such as pipeline inspection and maintenance, exploration of confined or hazardous spaces, cleaning of narrow and hard-to-reach areas, search and rescue operations, and environmental monitoring.

9. Conclusions

The paper investigates the dynamic behavior and locomotion characteristics of vibration-driven robots with wheeled chassis, focusing on the comparison of two types of vibration exciters: a solenoid-type actuator and a centrifugal (inertial) exciter. The research methodology involves 3D modeling using SolidWorks software to design the robots, numerical modeling in Mathematica software to simulate their motion and predict kinematic characteristics, and computer simulation in SolidWorks Motion software to validate the modeling results. The robots utilize overrunning clutches to ensure unidirectional wheel rotation and achieve forward motion through the principle of pure vibratory and vibro-impact locomotion. The influence of excitation frequency and operational parameters on the robot's speed, acceleration, and displacement is analyzed for both types of exciters. The results demonstrate the effectiveness of both solenoid and centrifugal exciters in achieving locomotion, with the centrifugal exciter generally providing lower speeds (approximately 56 mm/s) due to utilizing pure vibration excitation and the solenoid-type actuator offering larger speeds (approximately 60 mm/s) due to operating at vibro-impact conditions. The findings of this study are valuable for researchers and engineers working on the design and optimization of vibration-driven robots for various applications, including pipeline inspection, cleaning, and navigation in challenging environments.

[1] Korendiy V., Kachur O., Gursky V., Kotsiumbas O., Dmyterko P., Nikipchuk S., Danylo Y. Motion simulation and impact gap verification of a wheeled vibration-driven robot for pipelines inspection. Vibroengineering Procedia. **41**, 1–6 (2022).

[2] Korendiy V., Gursky V., Kachur O., Gurey V., Havrylchenko O., Kotsiumbas O. Mathematical modeling of forced oscillations of semidefinite vibro-impact system sliding along rough horizontal surface. Vibroengineering Procedia. **39**, 164–169 (2021).

[3] Nguyen V.-D., La N. T. An improvement of vibration-driven locomotion module for capsule robots. Mechanics Based Design of Structures and Machines. **50** (5), 1658–1672 (2020).

[4] Tian J., Afebu K. O., Wang Z., Liu Y., Prasad S. Dynamic analysis of a soft capsule robot self-propelling in the small intestine via finite element method. Nonlinear Dynamics. **111** (11), 9777–9798 (2023).

[5] Du Z., Fang H., Zhan X., Xu J. Experiments on vibration-driven stick-slip locomotion: A sliding bifurcation perspective. Mechanical Systems and Signal Processing. **105**, 261–275 (2018).

[6] Xu J., Fang H. Improving performance: recent progress on vibration-driven locomotion systems. Nonlinear Dynamics. **98** (4), 2651–2669 (2019).

[7] Nunuparov A., Becker F., Bolotnik N., Zeidis I., Zimmermann K. Dynamics and motion control of a capsule robot with an opposing spring. Archive of Applied Mechanics. **89** (10), 2193–2208 (2019).

[8] Li P., Jiang Z. Bifurcation analysis of stick-slip motion of the vibration-driven system with dry friction. Mathematical Problems in Engineering. **2018**, 2305187 (2018).

[9] Diao B., Zhang X., Fang H., Xu J. Bi-objective optimization for improving the locomotion performance of the vibration-driven robot. Archive of Applied Mechanics. **91** (5), 2073–2088 (2021).

[10] Diao B., Zhang X., Fang H., Xu J. Optimal control of the multi-module vibration-driven locomotion robot. Journal of Sound and Vibration. **527**, 116867 (2022).

[11] Nguyen K.-T., La N.-T., Ho K.-T., Ngo Q.-H., Chu N.-H., Nguyen V.-D. The effect of friction on the vibro-impact locomotion system: modeling and dynamic response. Meccanica. **56** (8), 2121–2137 (2021).

[12] Lee H.-S., Park S.-G., Hong M.-P., Lee H.-J., Kim Y.-S. A study on the manufacture of permanent magnet traction control valve for electronic stability control in electric vehicles. Applied Sciences. **11** (17), 7794 (2021).

[13] Korendiy V., Kachur O., Gursky V., Gurey V., Pelio R., Kotsiumbas O. Experimental investigation of kinematic characteristics of a wheeled vibration-driven robot. Vibroengineering Procedia. **43**, 14–20 (2022).

[14] Korendiy V., Kotsiumbas O., Borovets V., Gurey V., Predko R. Mathematical modeling and computer simulation of the wheeled vibration-driven in-pipe robot motion. Vibroengineering Procedia. **44**, 1–7 (2022).

[15] Loukanov I. A., Stoyanov S. P. Experimental determination of dynamic characteristics of a vibration-driven robot. IOSR Journal of Mechanical and Civil Engineering. **12** (4), 62–73 (2015).

[16] Loukanov I. A., Vitliemov V. G., Ivanov I. V. Dynamics of a mobile mechanical system with vibration propulsion (VibroBot). International Journal of Research in Engineering and Science. **4** (6), 44–51 (2016).

[17] Loukanov I. A., Vitliemov V. G., Ivanov I. V. Dynamics of a vibration-driven one-way moving wheeled robot. IOSR Journal of Mechanical and Civil Engineering. **13** (3), 14–22 (2016).

[18] Chavez J., Böhm V., Becker T. I., Gast S., Zeidis I., Zimmermann K. Actuators based on a controlled particle-matrix interaction in magnetic hybrid materials for applications in locomotion and manipulation systems. Physical Sciences Reviews. **7** (11), 1263–1290 (2022).

[19] Demarchi A., Farɜoni L., Pinto A., Lang R., Romero R., Silva I. Modelling a solenoid's valve movement. Lecture Notes in Computer Science. **11175**, 290–301 (2018).

[20] Korendiy V., Kachur O. Locomotion characteristics of a wheeled vibration-driven robot with an enhanced pantograph-type suspension. Frontiers in Robotics and AI. **10**, 1239137 (2023).

[21] Korendiy V., Lanets O., Kachur O., Dmyterko P., Kachmar R. Determination of inertia-stiffness parameters and motion modelling of three-mass vibratory system with crank excitation mechanism. Vibroengineering Procedia. **36**, 7–12 (2021).

[22] Badr M. F. Modelling and simulation of a controlled solenoid. IOP Conference Series: Materials Science and Engineering. **433** (1), 012082 (2018).

[23] El-Derini M. N. Mathematical model of a solenoid for energy and force calculations. Journal of Physics D: Applied Physics. **17** (3), 503–508 (1984).

[24] Peng Z., Chen L., Wei L., Gao W., Yu Q., Ai C. Analysis and identification of a dynamic model for proportional solenoid. IEEE Access. **9**, 92651–92660 (2021).

[25] Korendiy V., Lanets O., Kachur O., Dmyterko P., Kachmar R. Determination of inertia-stiffness parameters and motion modelling of three-mass vibratory system with crank excitation mechanism. Vibroengineering Procedia. **36**, 7–12 (2021).

[26] Korendiy V., Gursky V., Kachur O., Dmyterko P., Kotsiumbas O., Havrylchenko O. Mathematical model and motion analysis of a wheeled vibro-impact locomotion system. Vibroengineering Procedia. **41**, 77–83 (2022).

[27] Korendiy V., Krot P., Kachur O., Gurskyi V. Analyzing the locomotion conditions of a wheeled vibration-driven system with a V-shaped suspension. Advances in Design, Simulation and Manufacturing VII (DSMIE 2024). 153–163 (2024).

[28] Hosseini A. M., Arzanpour S., Golnaraghi F., Parameswaran A. M. Solenoid actuator design and modeling with application in engine vibration isolators. Journal of Vibration and Control. **19** (7), 1015–1023 (2013).

[29] Yang L., Gao T., Du X., Zhai F., Lu C., Kong X. Electromagnetic characteristics analysis and structure optimization of high-speed fuel solenoid valves. Machines. **10** (10), 964 (2022).

[30] Fang H., Wang K. W. Piezoelectric vibration-driven locomotion systems – Exploiting resonance and bistable dynamics. Journal of Sound and Vibration. **391**, 153–169 (2017).

[31] Korendiy V., Kachur O., Litvin R., Nazar I., Brytkovskyi V., Nikipchuk S., Ostashuk M. Simulation and experimental testing of locomotion characteristics of a vibration-driven system with a solenoid-type actuator. Vibroengineering Procedia. **56**, 29–35 (2024).

Математичне моделювання та комп'ютерне симулювання умов руху роботів з вібраційним приводом

Корендій В., Качур О., Киричук В., Маркович Б.

Національний університет "Львівська політехніка", вул. С. Бандери, 12, 79013, Львів, Україна

У цій статті досліджено динамічну поведінку та характеристики руху роботів з вібраційним приводом та колісним шасі, зосереджуючись на порівнянні двох типів вібраційних збудників коливань: електромагнітного актуатора та відцентрового (інерційного) віброзбудника. Методологія дослідження включає 3D-моделювання в програмному забезпеченні SolidWorks для проєктування роботів, чисельне моделювання в Mathematica для імітації їхнього руху та прогнозування кінематичних характеристик, а також комп'ютерне симулювання в SolidWorks Motion для валідації результатів математичного моделювання. Роботи використовують обгінні муфти для забезпечення однонапрямленого обертання коліс та досягнення поступального руху за принципами чисто вібраційного та віброударного збудження. Проаналізовано вплив частоти збудження та інших експлуатаційних параметрів на швидкість, пришвидшення та переміщення робота для обох типів віброзбудників. Результати демонструють ефективність як електромагнітних, так і відцентрових віброзбудників у досягненні необхідних параметрів руху, причому відцентровий віброзбудник загалом забезпечує нижчі швидкості руху робота через використання чисто вібраційного збудження, тоді як електромагнітний актуатор забезпечує більші швидкості завдяки роботі у віброударних режимах. Результати цього дослідження можуть бути цінними для дослідників та інженерів, які працюють над проєктуванням та оптимізацією роботів із вібраційним приводом для різних застосувань, включаючи інспектування і чищення трубопроводів та переміщення в складних умовах та середовищах (наприклад, поміж завалами будинків).

Ключові слова: *математична модель; комп'ютерне симулювання; електромагнітний віброзбудник; незбалансований ротор; характеристики руху; динамічна схема; мобільна робототехніка; колісне шасі; обгінна муфта.*